Applied Computer Science, vol. 18, no. 2, pp. 43–55
doi: 10.35784/acs-2022-12

Submitted: 2022-03-28 | Revised: 2022-05-16 | Accepted: 2022-05-21

Keywords: finite element method (FEM), post-buckling, progressive failure analysis (PFA), delamination, cohesive zone model (CZM)

Blazej CZAJKA [0000-0002-0870-5334]*, *Patryk ROZYLO* [0000-0003-1997-3235]*, *Hubert DEBSKI* [0000-0002-1916-8896]*

STABILITY AND FAILURE OF THIN-WALLED COMPOSITE STRUCTURES WITH A SQUARE CROSS-SECTION

Abstract

This paper is devoted to the analysis of the stability and load-carrying capacity of thin-walled composite profiles in compression. The specimens reflect elements made of carbon fibre reinforced laminate (CFRP). Thin-walled columns with a square cross-section were made from 4 layers of composite in 3 different combinations of layer arrangements. Advanced numerical analyses have been carried out. In the first stage of the study, a buckling analysis of the structure was performed. In further numerical simulations, two advanced models were used simultaneously: the Progressive Failure Analysis (PFA) and the Cohesive Zone Model (CZM). The results showed significant differences between the critical load values for each layer configuration. The forms of buckling and the areas of damage initiation and evolution were also dependent on the applied layup.

1. INTRODUCTION

Thin-walled structures have been a very common type of load-bearing structure in many sectors of industry for many years. They have a major role to play in the construction of aircraft, vehicles and modern buildings. Thin-walled structural elements with different cross-sections, both open and closed (stringers, frames, profiles), are used to transfer loads. Due to the favourable weight/strength ratio, especially for aeronautical structures, more and more components are being manufactured from composite materials in favour of traditional engineering materials. One of the widely used composites is the continuous carbon fibre reinforced polymer (CFRP) laminate. It is also characterised by chemical and corrosion resistance and high fatigue strength (Chung, 1994). It is used in aviation to manufacture many responsible parts such as fuselage and landing gear components, airframes, and helicopter blades (Freeman, 1993). The most commonly used method of manufacturing critical composite parts is the autoclave technique (Campbell, 2004, 2006), which ensures high strength of these parts, repeatability of the manufacturing process, as well as low

* Lublin University of Technology, Faculty of Mechanical Engineering, Department of Machine Design and Mechatronics, Lublin, Poland, blazej.czajka@pollub.edu.pl, p.rozylo@pollub.pl, h.debski@pollub.pl

internal porosity of the composite material. Thin-walled load-bearing elements during exploitation should be used in the stable range, which is the subject of many scientific papers (Berardi, Perrella, Feo & Cricri, 2017; Fascetti, Feo, Nistici & Penna, 2016; Kubiak, Kolakowski, Swinarski, Urbaniak & Gliszczynski, 2016).

Buckling of a structural member may occur due to, for example, compressive loading (Debski, Teter, Kubiak & Samborski, 2016). This results in operation of the structure in the coverage range and accelerated failure. During stable working, thin-walled composite structures show the possibility of continuing to carry the axial compressive load, even after the buckling phenomenon has occurred (Koiter, 1963; Kubiak, Kolakowski, Swinarski, Urbaniak & Gliszczynski, 2016; Singer, Arbocz & Weller, 2000). As shown by previous studies (Debski, Rozylo, Gliszczynski & Kubiak, 2019; Falkowicz, Mazurek, Rozylo, Wysmulski & Smagowski, 2016; Wysmulski, Debski, Rozylo & Falkowicz, 2016), they have a large reserve of load-carrying capacity as long as the buckling is elastic in nature and the post-buckling equilibrium path remains stable. Therefore, the study of stability and the load-carrying capacity of thin-walled composite structures, requires analysis both in the state before and after the occurrence of loss of stability (Paszkiewicz & Kubiak, 2015; Rozylo, Debski, Wysmulski & Falkowicz, 2018). The analysis of composite structures determines the study of the full load range up to failure (Abrate, 1998) and the description of the phenomena of initiation and evolution of failure (Liu, Gu, Peng & Zheng, 2015). Many papers also demonstrate the ability of the described structures to carry loads after failure of the first laminate layer, as well as significant differences in limit load values, depending on the configuration of the composite layers (Debski, Teter, Kubiak & Samborski, 2016). Composite elements are characterised by a more complex failure mechanism than traditional materials (e.g. metals). They may fail as a result of tension or compression of the fibres, tension or compression of the matrix, and shear between layers (Camanho & Matthews, 1999; Lapczyk & Hurtado, 2007). This requires that experiments be conducted using several measurement methods simultaneously and that advanced failure models be applied during numerical simulations. Numerical analyses allowing observation of failure initiation and evolution phenomena are usually carried out using the progressive failure analysis (PFA) model (Camanho & Matthews, 1999; Lapczyk & Hurtado, 2007), whereas the cohesion zone model (CZM) is usually applied to describe the delamination phenomenon (Liu, Gu, Peng & Zheng, 2015).

In most of the published works, the authors focus only on open cross-sections. The current study is based on a comparison of thin-walled columns with a square cross-section (closed cross-section) prepared in 3 different laminate layer configurations. Furthermore, the numerical simulations have been carried out in a more detailed way than in previously published works. Both PFA and CZM numerical models were used simultaneously. Furthermore, the cohesion zones were used globally. Previous work uses cohesive zones only at delamination locations on real specimens during experimental tests. This definitely simplifies the model and may lead to the omission of delamination phenomena in other areas of the elements. The present work is devoted exclusively to numerical analysis as a preliminary to further research on closed sections. In order to validate the simulation results obtained, experimental tests are planned to be carried out in the next stages.

2. METHOD

2.1. Object of research

In this study, columns made of a closed square profile with a height equal to 250 mm were examined. The internal side length of the square was 40 mm. For a better representation of the real specimens, a corner rounding was used. The composite was made of 4 layers of laminate, each 0.1 mm thick. The exact dimensions of the model are shown in Figure 1. In this paper, 3 different configurations of the arrangement of the laminate layers were analysed:

- P1 – [0/90/90/0],
- P2 – [90/0/0/90],
- P3 – [45/0/0/45].

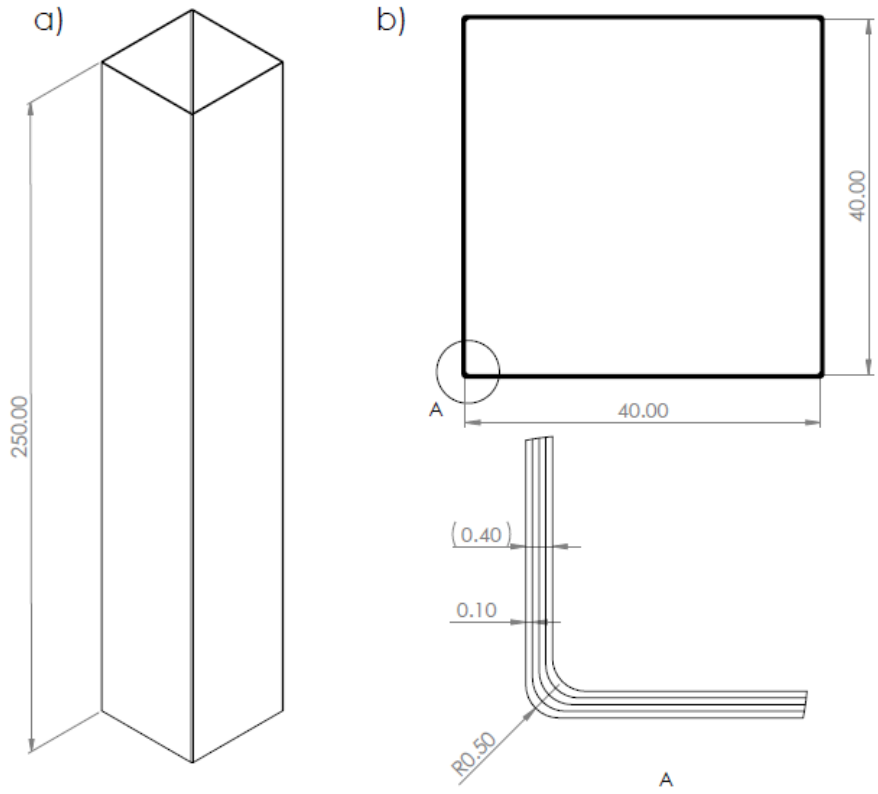

Fig. 1. Test specimen: a) specimen height, b) cross-sectional parameters

The specimens were made of carbon-epoxy laminate (CFRP). The used mechanical and strength properties are similar to those found in the literature (Rozylo, Debski, Wysmulski & Falkowicz, 2018) and shown in Table 1.

Tab. 1. Material properties of CFRP

Symbol	Property	Value	Unit
E_1	Young's modulus (along fibres)	130000	MPa
E_2	Young's modulus (perpendicular to fibres)	6500	
G_{12}	Kirchhoff modulus	5000	
ν_1	Poisson's coefficient	0.3	–
F_{T1}	Tensile Strength (along fibres)	2000	MPa
F_{C1}	Compressive Strength (along fibres)	100	
F_{T2}	Tensile Strength (perpendicular to fibres)	1500	
F_{C2}	Compressive Strength (perpendicular to fibres)	50	
F_{12}	Shear Strength	100	

2.2. Numerical analysis

The simulations were carried out based on the finite element method (FEM) using the Abaqus software. The first part of the research consisted in the analysis of the buckling of the structure. The Progressive Failure Analysis (PFA) and Cohesive Zone Model (CZM) were used to analyse post-buckling, loss of load-carrying capacity and delamination.

The first stage of the research was to solve the eigenproblem based on the minimum potential energy criterion. This allowed to obtain the buckling form and the critical load value. The critical load value was defined using the equation:

$$\left(K_0^{NM} + \lambda_i K_\Delta^{NM}\right) v_i^M = 0 \tag{1}$$

where: K_0^{NM} represents the stiffness matrix (corresponding to the base state), which includes the effects of preloads (P^N), K_Δ^{NM} denotes the differential initial stress as well as load stiffness matrix due to the incremental loading pattern (Q^N), λ_i represent the eigenvalues, v_i^M constitute the buckling mode shapes – eigenvectors, ^{M} and ^{N} refer to degrees of freedom M and N (of the whole model), $_i$ refers to the $_i$th mode of buckling. The critical buckling loads are $P^N + \lambda_i Q^N$. Furthermore, v_i^M constitute normalized vectors (and do not represent real magnitudes of deformation at critical load).

Then, simulations of non-linear loss of stability and load-carrying capacity of the structure were performed. The study also included the phenomenon of delamination occurring between the composite layers. In order to better represent the real phenomena, imperfections of the model from the form of buckling obtained in the first stage of research were used.

The preparation of the computational models involved making each laminate layer separately and then adding contact relations between them with the properties of cohesive layers. This made it possible to observe the delamination phenomenon in the whole model.

During the test, thin-walled composite columns were subjected to compressive loads over the full range up to failure. Two non-deformable plates were added to the ends of each column in order to best represent real conditions. Contact relationships were established between the composite columns and the plates in the normal and tangential directions. One of the plates (bottom plate) was fully fixed by removing all degrees of freedom. The upper plate was fixed in all directions except the direction along the height of the test specimen (Z axis). A compressive force was applied to this plate (fig. 2).

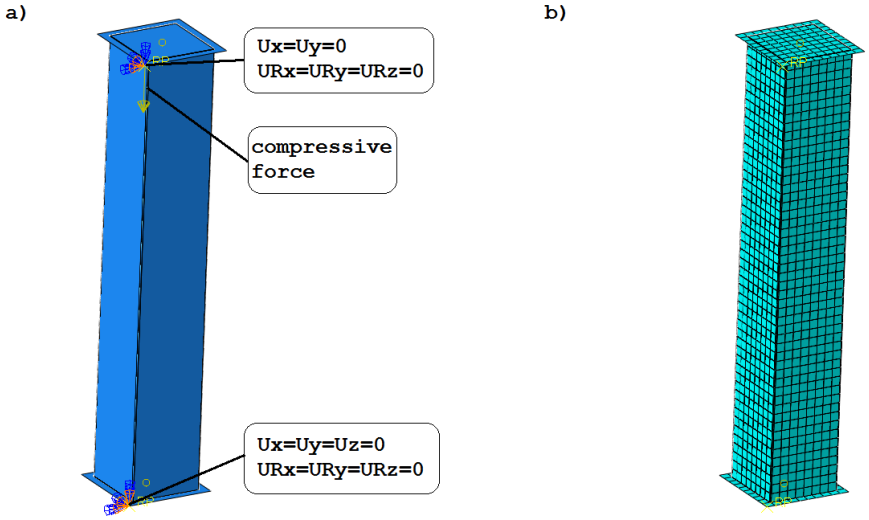

Fig. 2. Test specimen: a) constraints and loading, b) discrete model

The prepared models were discretised. Non-deformable, four-node elements with a linear shape function (R3D4) were used for the support plates. SC8R elements (eight-node shell elements with linear shape function) were used for the laminate layers. The numerical model for each layer layout consisted of 200 R3D4 elements, 8000 SC8R elements and 16562 nodes. A view of the discrete model is shown in Figure 2.

3. RESULTS

3.1. Buckling analysis

The analysis of the buckling of the structure showed significant differences between the studied arrangements of composite layers. The differences can be seen both in the values of critical loads causing buckling of the composite columns and in the form of buckling of the structure.

As shown in the graph (Fig. 3.), the obtained buckling load for the K3 configuration was the highest and amounted to about 804 N. The loss of stability for K1 and K2 occurred at similar load values of 703 N and 694 N, respectively. The load for the K3 configuration was therefore 14% and 16% higher respectively. This suggests that the use of layers at 45 degrees to the compressive force reinforces the structures and increases the buckling strength.

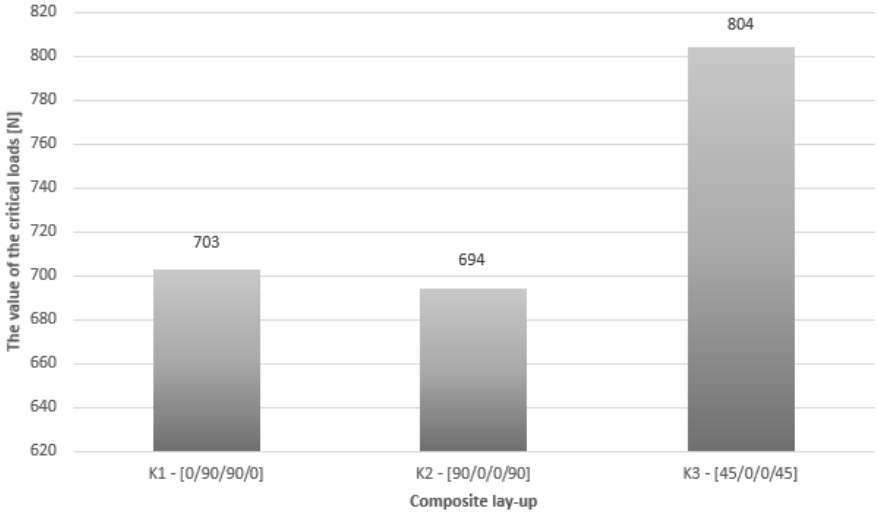

Fig. 3. Critical load values

The buckling forms, shown in Figure 4, are completely different depending on the layup. For configuration K1, 4 half-waves occur on each wall. The appearance of the half-waves is symmetrical with respect to the planes passing through the centres of the opposite edges of the cross-section. For the K2 configuration there is also symmetry, but the number of occurrence of half-waves has significantly increased to 9 on each wall. A completely different form of buckling is visible on the specimen in the K3 configuration. There are 5 half-waves on two of the walls and 7 half-waves on the other two walls. There is no symmetry as seen in the previous specimens. The half-waves are arranged at an angle of 45 degrees, according to the arrangement of fibres in the outer and inner layer of the composite.

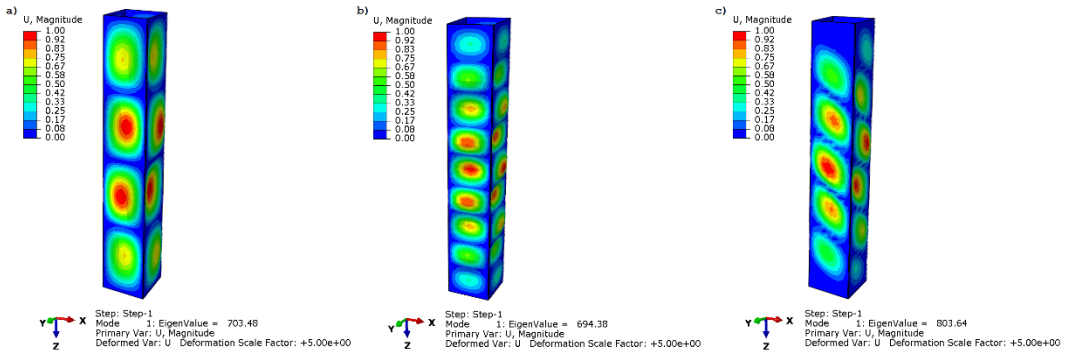

Fig. 4. Buckling view for layer arrangements: a) K1, b) K2, c) K3

3.2. Damage initiation

Damage initiation was analysed using two criteria: Tsai-Wu and Hashin. The results obtained with these criteria did not show much difference from each other. The biggest deviation was recorded for the K2 configuration, but it did not exceed 3.5%. Achieved values

of damage initiation forces and their differences between the used criteria are summarised in Table 2. In K1 and K2 configurations, damage initiation occurred at similar loads (for selected criteria). Opposite to buckling, configuration K3 was found to be the least strong at the time of damage initiation. The damage initiation load for K3 compared to the other configurations was about 16% lower according to the Tsai-Wu criterion and about 18% lower according to the Hashin criterion. It is important to emphasise that the failure initiation loads are as much as 5 to 7 times higher than the critical loads causing buckling of the structure. According to the Hashin criterion, the damage initiation occurred as a result of matrix tension – in the case of K1 configuration, and matrix compression in the case of K2 and K3 configurations.

Tab. 2. Load values for damage initiation (Tsai-wu and Hashin criteria)

Composite layup	Damage initiation forces [N]		Difference	
	Tsai-Wu criterion	Hashin criterion	[N]	[%]
K1	4995	5129 (matrix tension)	134	2.68
K2	4905	5128 (matrix compression)	168	3.43
K3	4218	4218 (matrix compression)	0	0

The distributions of damage initiation obtained with the Tsai-Wu criterion are shown in Figure 5. The analysis by using this criterion shows that initiation for each of the systems occurs on the inner layer, and only for the K1 configuration also on the outer layer.

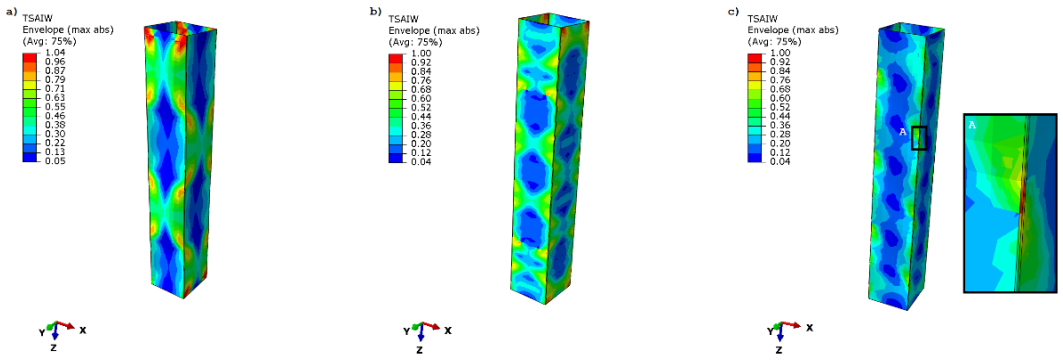

Fig. 5. Distribution maps of damage initiation on layer 1 – Tsai-Wu criterion: a) K1, b) K2, c) K3

For the Hashin criterion, for all configurations the damage initiation is visible on the inner layer. A view of the damage initiation distribution according to this criterion is shown in Figure 6.

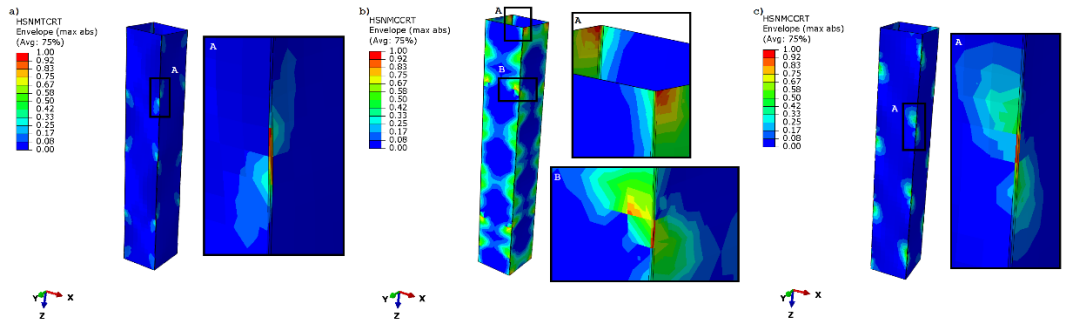

Fig. 6. Distribution maps of damage initiation on layer 1 – Hashin criterion: a) K1, b) K2, c) K3

In general, the areas exposed to damage initiation are the corners of the tested columns and the buckling half-wave hinge locations at the edges of the element. The areas of damage initiation are identical except the layup configuration K1. For this layup, according to the Tsai-Wu criterion, the corners are the locations of damage initiation. In the case of analysis using the Hashin criterion, damage initiation occurs at the edges of the element at the half-wave inflection point. Low values for this criterion are observed in the corners.

3.3. Damage evolution

The application of progressive failure analysis (PFA) has allowed the study of the areas of occurrence, the failure mechanism and the loads at the time of damage evolution. The damage evolution occurred in 1 layer of the composite for each of the investigated configurations. The areas were identical to those observed at failure initiation (Fig. 7).

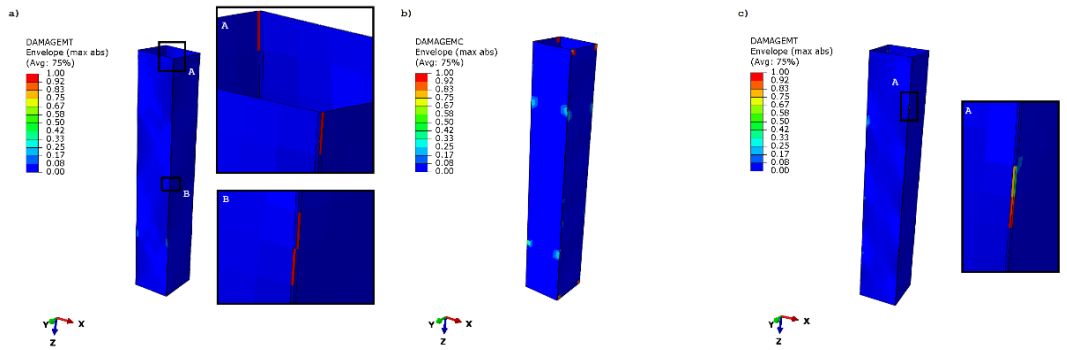

Fig. 7. Areas of damage evolution in different layups: a) K1 – DAMAGEMT, b) K2 – DAMAGEMC, c) K3 - DAMAGEMT

For the K1 and K3 layer configurations, the damage occurred by tension of the composite matrix (DAMAGEMT), while for K2 it occurred by compression of the matrix (DAMAGEMC). During the tests carried out for all configurations, matrix damage occurred in both tension and compression before the tested structure lost its load-carrying capacity. For configurations K2 and K3 the fibre damage (DAMAGEFC) was also observed in compression but after the loss of load-carrying capacity. The fibre failure due to tension (DAMAGEFT) and, in the case of K1, due to compression were not reached during the tests.

The loads that caused the reach of the individual parameters are summarised in the table below (Tab. 3).

Tab. 3. Load values at damage evolution

Composite layup	Load values [N]			
	DAMAGEMC	DAMAGEMT	DAMAGEFC	DAMAGEFT
K1	5602	**5518**	–	–
K2	**5557**	5826	5116*	–
K3	6471	**5486**	6321*	–

* – evolution has taken place after the loss of load-carrying capacity

3.4. Delamination

Observation of the delamination phenomenon was possible by using the cohesive zone model (CZM). Both the initiation (CSMAXSCRT) and evolution of delamination (CSDMG) occurred in areas close to the initiation and evolution of failure. The main areas exposed to delamination were the corners of the elements and the half-wave inflection points at their edges. The locations of occurrence between layers 3 and 4 for the K2 configuration are shown in Figure 8.

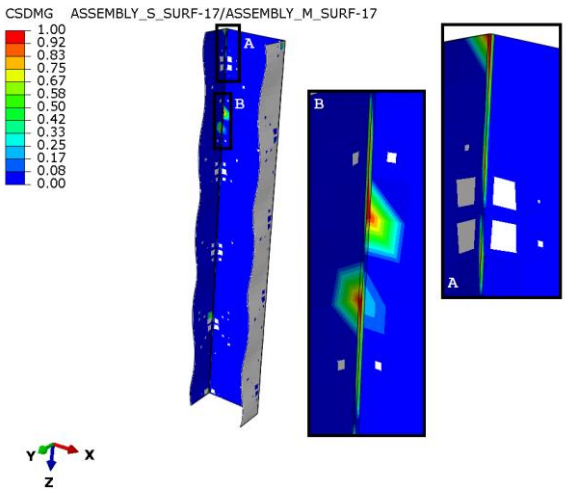

Fig. 8. Locations of delamination between layers 3 and 4 - K2 configuration

The applied numerical model allowed for excellent visualisation of the delamination phenomenon for the tested samples. It is especially visible in the corners of the investigated composite columns. The following figure (Fig. 9) shows a view of delamination for the K2 configuration.

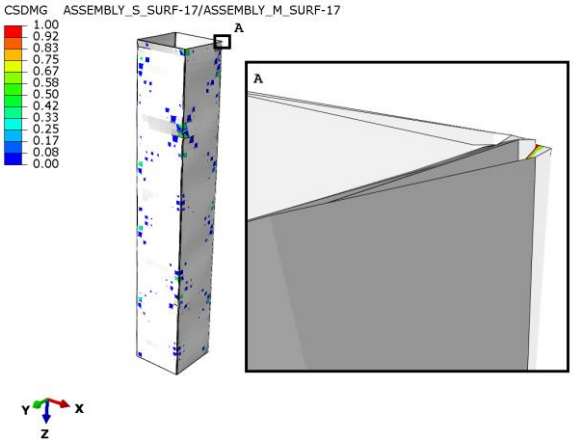

Fig. 9. Delamination view for K2 configuration

For each of the tested configurations, delamination initiation between at least two layers occurred before damage initiation. Delamination initiation was achieved for all specimens between each layer during the tests. Each of them occurred before the loss of load-carrying capacity of the tested structures. The delamination evolution was not achieved only between layers 2 and 3 in the K1 configuration. For each configuration, at least between two of the layers delamination occurred before the loss of load-carrying capacity of the structure. The occurrence of the phenomenon in the load-carrying area of composite structures confirms the importance of its analysis. This may allow better prediction of the behaviour of real structures made of laminates.

3.5. Equilibrium paths and loss of load-carrying capacity

By carrying out the study over the full load range, the moment of loss of bearing capacity was obtained. In order to analyse this phenomenon, equilibrium paths were determined. They allow for a convenient analysis of the sequence of occurrence of particular phenomena during compression of the tested specimens. The equilibrium path for the K3 configuration is shown in Figure 10.

In the presented configuration, delamination initiation occurred at forces of 3083 N and 3257 N. Subsequently, damage initiation occurred at a force of 4218 N (according to Tsai_Wu and Hashin's criterion). Although this point was exceeded, the structure still carried the load, which increased continuously. Successively, the matrix damage evolution took place by tension, compression and then the delamination between layers 1 and 2, and layers 3 and 4 occurred. Loss of load-carrying capacity occurred only when a load of 6642 N was reached. In the same calculation step, delamination evolved between layers 2 and 3.

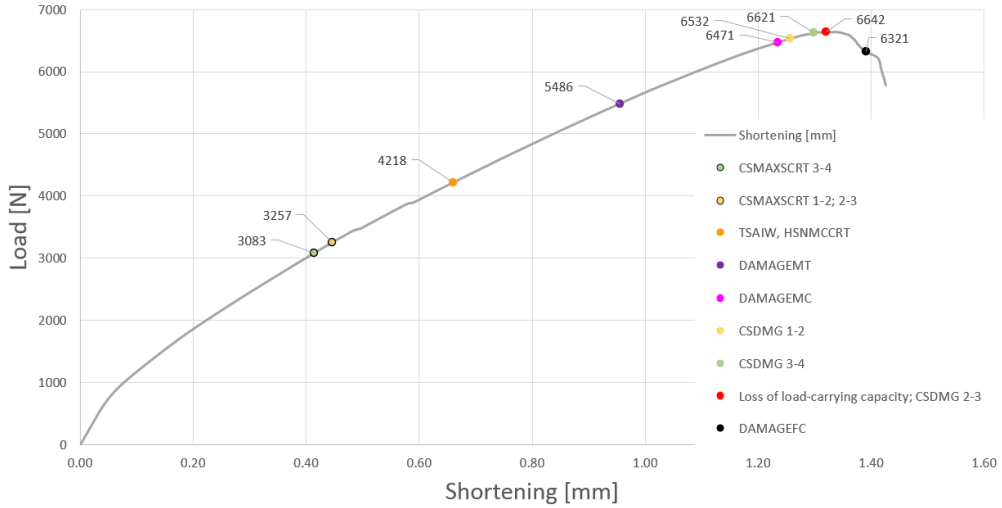

Fig. 10. Equilibrium path – K3 layup

The load causing loss of load-carrying capacity for all the tested composites was significantly higher than the load causing damage initiation. For the K3 configuration, this difference was as high as 2424 N, which is about 57% of the value of the damage initiation load. For K1 and K2 configurations the differences were smaller but also significant. They were 622 N (12%) and 922 N (19%), respectively. The K3 configuration was characterized by the highest load-carrying capacity (Fig. 11).

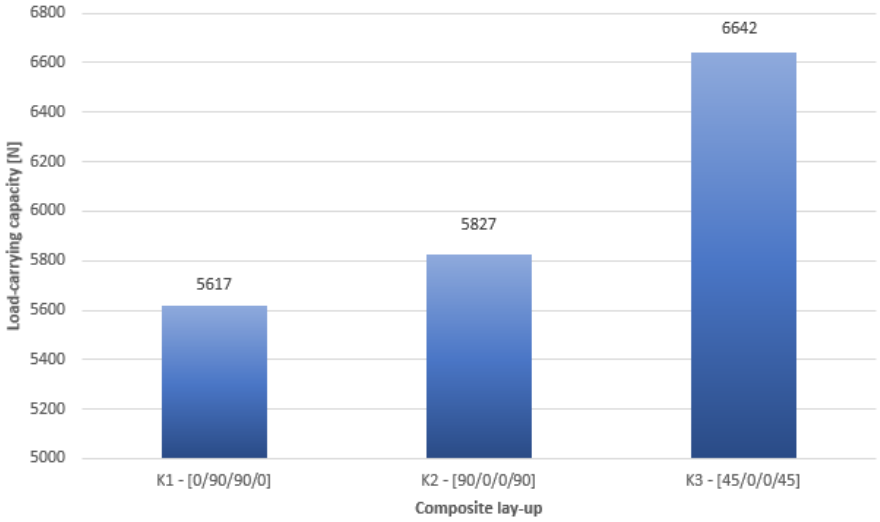

Fig. 11. Load-carrying capacity for different configurations

4. CONCLUSIONS

The numerical analyses carried out allowed comparison of composite thin-walled columns with square cross-sections and various arrangements of laminate layers. They also provided a preliminary study of the stability and load-carrying capacity of compression composite profiles with closed cross-sections. The conducted research results in the following conclusions:

- the buckling analysis of thin-walled structures with square cross-section is possible by using FEM and solving the eigenproblem,
- applying the PFA model allows to thoroughly analyse the post-buckling behaviour of composite columns with square cross-section,
- the Cohesive Zone Model (CZM) is a useful method to analyse the phenomenon of delamination in composite structures with closed cross-section,
- the arrangement of composite layers has a significant influence on buckling, initiation and evolution of damage, delamination, as well as the load-carrying capacity of composite structures,
- the sample with layers arranged at the angle of 45 degrees was characterised by the lowest stability of the structure, but at the same time the highest load-carrying capacity,
- for all tested configurations the phenomenon of delamination occurred before the loss of load-carrying capacity, which confirms the importance of its investigation,
- each of the tested specimens lost its load-carrying capacity at a load significantly higher than the load occurring at the damage initiation.

Future experimental research using a universal testing machine is planned as part of the project No. 2021/41/B/ST8/00148 (National Science Centre, Poland). The study of the composite structure damage will be performed based on acoustic emission method and microscopic analysis. A digital microscope with a mobile head will be used to record the forms of failure during compression of the specimens.

Funding

The publication was financed by Grant – Lublin University of Technology Doctoral School – Błażej Czajka.

Acknowledgments

The research has been conducted under project No. 2021/41/B/ST8/00148 (National Science Centre, Poland)

REFERENCES

Abrate, S. (1998). *Impact on Composite Structures.* Cambridge University Press.

Berardi, V. P., Perrella, M., Feo, L., & Cricri, G. (2017). Creep behavior of GFRP laminates and their phases: Experimental investigation and analytical modelling. *Composites Part B: Engineering*, *122*, 136–144. https://doi.org/10.1016/j.compositesb.2017.04.015

Camanho, P. P., & Matthews, F. L. (1999). A Progressive Damage Model for Mechanically Fastened Joints in Composite Laminates. *Journal of Composite Materials*, *33*(24), 2248–2280. https://doi.org/10.1177%2F002199839903302402

Campbell, F. C. (2004). *Manufacturing Processes for Advanced Composites.* Elsevier B.V.

Campbell, F. C. (2006). *Manufacturing Technology for Aerospace Structural Materials.* Elsevier Ltd.

Chung, D. D. L. (1994). *Carbon Fiber Composites.* Elsevier Inc.

Debski, H., Rozylo, P., Gliszczynski, A., & Kubiak, T. (2019). Numerical models for buckling, postbuckling and failure analysis of pre-damaged thin-walled composite struts subjected to uniform compression. *Thin-Walled Structures*, *139*, 53–65. https://doi.org/10.1016/j.tws.2019.02.030

Debski, H., Teter, A., Kubiak, T., & Samborski, S. (2016). Local buckling, post-buckling and collapse of thin-walled channel section composite columns subjected to quasi-static compression. *Composite Structures*, *136*, 593–601. https://doi.org/10.1016/j.compstruct.2015.11.008

Falkowicz, K., Mazurek, P., Rozylo, P., Wysmulski, P., & Smagowski, W. (2016). Experimental and numerical analysis of the compression thin-walled composite plate. *Advances in Science and Technology Research Journal*, *10*(31), 177–184. https://doi.org/10.12913/22998624/64063

Fascetti, A., Feo, L., Nisticò, N., & Penna, R. (2016). Web-flange behavior of pultruded GFRP I-beams: A lattice model for the interpretation of experimental results. *Composites Part B: Engineering*, *100*, 257–269. https://doi.org/10.1016/j.compositesb.2016.06.058

Freeman, W. T. (1993). The use of composites in aircraft primary structure. *Composites Engineering*, *3*(7–8), 767–775. https://doi.org/10.1016/0961-9526(93)90095-2

Koiter, W. (1963). *Elastic Stability and Post Buckling Behavior in Nonlinear Problems.* University of Wisconsin Press.

Kubiak, T., Kolakowski, Z., Swinarski, J., Urbaniak, M., & Gliszczynski, A. (2016). Local buckling and post-buckling of composite channel-section beams – Numerical and experimental investigations. *Composites Part B: Engineering*, *91*, 176–188. https://doi.org/10.1016/j.compositesb.2016.01.053

Lapczyk, I., & Hurtado, J. A. (2007). Progressive damage modeling in fiber-reinforced materials. *Composites Part A: Applied Science and Manufacturing*, *38*(11), 2333–2341. https://doi.org/10.1016/j.compositesa.2007.01.017

Liu, P. F., Gu, Z. P., Peng, X. Q., & Zheng, J. Y. (2015). Finite element analysis of the influence of cohesive law parameters on the multiple delamination behaviors of composites under compression. *Composite Structures*, *131*, 975–986. https://doi.org/10.1016/j.compstruct.2015.06.058

Paszkiewicz, M., & Kubiak, T. (2015). Selected problems concerning determination of the buckling load of channel section beams and columns. *Thin-Walled Structures*, *93*, 112–121. https://doi.org/10.1016/j.tws.2015.03.009

Rozylo, P., Debski, H., Wysmulski, P., & Falkowicz, K. (2018). Numerical and experimental failure analysis of thin-walled composite columns with a top-hat cross section under axial compression. *Composite Structures*, *204*, 207–216. https://doi.org/10.1016/j.compstruct.2018.07.068

Singer, J., Arbocz, J., & Weller, T. (1998). *Buckling Experiments: Experimental Methods in Buckling of Thin-Walled Structures, Volume 1: Basic Concepts, Columns, Beams and Plates.* John Wiley & Sons Inc.

Wysmulski, P., Debski, H., Rozylo, P., & Falkowicz, K. (2016). A study of stability and post-critical behaviour of thin-walled composite profiles under compression. *Eksploatacja i Niezawodnosc-Maintenance and Reliability*, *18*(4), 632–637. http://dx.doi.org/10.17531/ein.2016.4.19